Spin noise of itinerant fermions

Šimon Kos,[1,2,3,*] Alexander V. Balatsky,[3,4] Peter B. Littlewood,[2] and Darryl L. Smith[3]

[1]*Department of Physics, University of West Bohemia, Univerzitní 22, 306 14 Plzeň, Czech Republic*
[2]*Cavendish Laboratory, Cambridge University, Madingley Road, Cambridge CB3 0HE, United Kingdom*
[3]*Theoretical Division, Los Alamos National Laboratory, Los Alamos, New Mexico 87545, USA*
[4]*Center for Integrated Nanotechnologies, Los Alamos, New Mexico 87545, USA*

We develop a theory of spin-noise spectroscopy of itinerant, noninteracting, and spin-carrying fermions in different regimes of temperature and disorder. We use kinetic equations for the density matrix in spin variables. We find a general result with a clear physical interpretation, and discuss its dependence on temperature, the size of the system, and applied magnetic field. We consider two classes of experimental probes: (1) electron-spin-resonance-type measurements, in which the probe response to a uniform magnetization increases linearly with the volume sampled and (2) optical Kerr/Faraday rotation-type measurements, in which the probe response to a uniform magnetization increases linearly with the length of the light propagation in the sample but is independent of the cross section of the light beam. Our theory provides a framework for interpreting recent experiments on atomic gases and conduction electrons in semiconductors and provides a baseline for identifying the effects of interactions on spin-noise spectroscopy.

I. INTRODUCTION

Currently, there is much interest in studying the physics of nanoscale structures. In measurements of a response function by pump-probe experiments on systems of decreasing size, the signal decreases more rapidly than the noise, and thus the signal-to-noise ratio decreases with decreasing system size. The fluctuation-dissipation theorem, which relates a response function to a correlation function obtained from noise measurements, enables us to change this problem into a useful tool. An additional advantage of noise measurements is that they often disturb the system less than experiments that measure the response of the system to an external perturbation.

There have been a number of experiments studying spin properties of systems using spin noise. Spin noise has been measured in systems of spins whose position is *fixed in space*: atomic nuclei,[1] spin glasses,[2] magnetization modes in magnetoresistive heads,[3] and electrons and holes in self-assembled quantum dots.[4] There have also been recent measurements of spin noise of *itinerant* spins in hot atomic gases,[5–7] cold atomic gases,[8,9] in n-doped bulk GaAs,[10,11] and in n-doped GaAs quantum wells.[12] Localized spin-noise measurements on nanostructured systems using STM techniques have been discussed.[13,14] The experimental setup of spin-noise spectroscopy in semiconductors has been optimized in Ref. 15 and has been used to measure spatially resolved doping concentration in GaAs.[16] Motivated by these experiments with itinerant spins, we have developed a theory of spin noise of itinerant fermions in different regimes of temperature (degenerate/classical statistics) and disorder (ballistic/diffusive motion). We consider the case of noninteracting particles as a benchmark for comparison to experiments so that we can then identify the effects of interactions on spin noise. We find a general result that holds in the different regimes, which has a clear physical interpretation, and we show how it follows from kinetic equations for density matrix in spin variables. We consider two classes of

experimental probes: (1) electron-spin-resonance (ESR)-type measurements, in which the probe response to a uniform magnetization increases linearly with the volume sampled and (2) optical Kerr/Faraday rotation-type measurements, in which the probe response to a uniform magnetization increases linearly with the length of the light propagation in the sample but is independent of the cross section of the light beam.

The outline of the paper is as follows: in Sec. II, we present the general result and its interpretation. In Sec. III, we show how the noise spectrum behaves as a function of temperature, system size, and magnetic field. In Sec. IV, we present the derivation of the result from kinetic equations with details of calculations in some limiting cases presented in the Appendix B. In Sec. V, we present our Conclusions. The spin-noise power spectrum of spin J, which motivates our general result, is derived in the Appendix A.

II. GENERAL RESULT

In Fig. 1 we show the generic setup of the experiments considered. We study the noise of spin magnetization in the z direction in the presence of an applied constant magnetic field in the x direction that splits the two spin energy levels by the Larmor frequency ω_L. The purpose of the constant magnetic field is to shift the noise spectrum away from zero frequency. Noise measurements close to zero frequency are difficult because of the presence of ubiquitous $1/f$ noise. The magnetic field is chosen so that ω_L is larger than the linewidth of the spin-noise spectrum. For charged fermions, we neglect coupling of magnetic field to the orbital motion, that is, we consider the case when the cyclotron orbit is longer than the dimensions of the probed region. The system has thickness L in the z direction, which in the optical experiments is the direction of light propagation. The system is extended in the x-y direction. Noise in the part of the system with transverse size R and cross section $A \sim R^2$ is probed. In
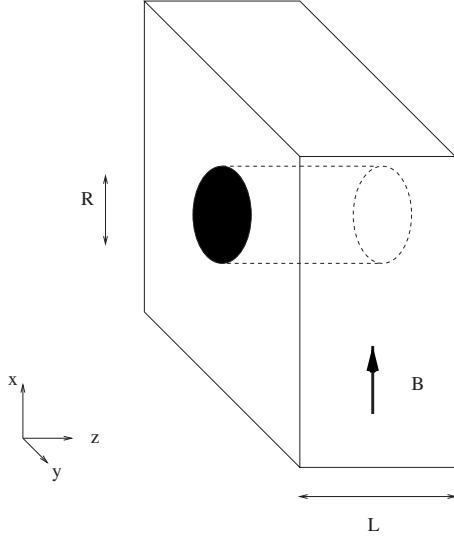
FIG. 1. Schematic view of the experimental setup. The experiment measures the noise of spin magnetization in the z direction in the presence of an applied constant magnetic field in the x direction that splits the two spin energy levels by the Larmor frequency ω_L. The system has thickness L in the z direction and is extended in the x-y direction. Noise in the part of the system with transverse size R and cross section $A \sim R^2$ is probed.

the setup we consider, these dimensions are larger than the fermion wavelength (Fermi wavelength in the degenerate case or thermal wavelength in the classical case). For a uniformly spin-polarized sample, the magnitude of the probe response in bulk measurements such as ESR scales as the volume of the probed region, that is, Signal $\propto R^2 L$. By contrast, for a uniformly spin-polarized sample, the magnitude of the probe response in optical Kerr/Faraday rotation measurements scales as the thickness L, but is independent of the cross-sectional area A, that is, Signal $\propto L$.

In general, the spin-noise experiment will measure the noise-power spectrum of a quantity Q proportional to the instantaneous electron spin polarization

$$Q(t) = C M_z(t) F_G, \qquad (1)$$

where $M_z(t)$ is the operator of the z component of the instantaneous electron spin polarization in the probed volume at time t, related to the spin-density operator $s_z(\mathbf{r}, t)$ by

$$M_z(t) = \int_{A \times L} d^3 r\, s_z(\mathbf{r}, t), \qquad (2)$$

where C is a fixed coupling constant and F_G is a geometric factor. For bulk measurement such as ESR, the geometric factor is unity. For optical Kerr/Faraday rotation measurements, the geometric factor is $1/A$. Hence, in either case, in order to calculate the spin-noise-power spectrum, we need the Fourier transform of the correlation function

$$S_{zz}(t_2 - t_1) = \frac{1}{2} \langle \{M_z(t_2), M_z(t_1)\} \rangle, \qquad (3)$$

where Here, $\{,\}$ denotes the anticommutator and $\langle \rangle$ is the equilibrium ensemble average.

In equilibrium, the fluctuation-dissipation theorem relates the noise power to the imaginary part of the corresponding susceptibility

$$S_{zz}(\omega) = -\coth\frac{\omega}{2T} \int_{A \times L} d^3 r_2 d^3 r_1 \chi_{zz}''(\mathbf{r}_2 - \mathbf{r}_1; \omega)$$

$$\simeq -\coth\frac{\omega}{2T} A \times L \chi_{zz}''(q = 1/R; \omega), \qquad (4)$$

where

$$\chi_{zz}(\mathbf{r}_2 - \mathbf{r}_1; t_2 - t_1) = -i\theta(t_2 - t_1)\langle [s_z(\mathbf{r}_2, t_2), s_z(\mathbf{r}_1, t_1)] \rangle. \qquad (5)$$

Here, χ_{zz} is the spin susceptibility and the double prime denotes the imaginary part.

We consider different regimes of temperature and particle motion. The calculations for the various cases are given in Sec. IV. The results of the calculation in all these cases have the following general form:

$$S_{zz}(\omega) \simeq \frac{\pi}{2}\coth\frac{\omega_L}{2T}\frac{M_x^{(0)}}{g(t_{tr}^{-1}, \tau_s^{-1})}f\left(\frac{\omega - \omega_L}{g(t_{tr}^{-1}, \tau_s^{-1})}\right). \qquad (6)$$

Here, $M_x^{(0)}$ is the equilibrium magnetization of the probed region caused by the constant magnetic field in the x direction, t_{tr} is the travel time it takes the spin-carrying fermion to move across the probed region (distance R), τ_s is the spin-decay time (in the direction perpendicular to the applied magnetic field, that is, T_2 in case T_1 and T_2 are different), f is a function of unit height and width, peaked at zero, and g is a function whose value is approximately equal to the greater of the two arguments

$$g(t_{tr}^{-1}, \tau_s^{-1}) \simeq \max(t_{tr}^{-1}, \tau_s^{-1}). \qquad (7)$$

The detailed form of the functions f and g depends on temperature and disorder. The form of the functions f and g for the various cases will be discussed in Sec. IV. Equation (6) is the main result of this paper. Its form agrees with the spin-noise-power spectrum of a single spin J—see Appendix A.

In Eq. (6), for ballistic transport

$$t_{tr} = R/v, \qquad (8)$$

where v is the Fermi velocity $\sqrt{2E_F/m}$ in the degenerate regime $T \ll E_F$ or the thermal velocity $\sqrt{2T/m}$ for $T \gg E_F$. For diffusive transport

$$t_{tr} = R^2/D, \qquad (9)$$

where D is the diffusion constant.

In Fig. 2, we show the schematic behavior of the spin-noise-power spectrum $S_{zz}(\omega)$. It is peaked at the Larmor frequency ω_L. Its width is approximately equal to the larger of the inverse travel time t_{tr}^{-1} and the inverse spin-flip time τ_s^{-1}. The height is given by the magnetization $M_x^{(0)}$ multiplied by the thermal factor $\coth \omega_L/2T$ and divided by the width.

The result in Eq. (6) has a simple physical interpretation. The scale of the response in the z direction is set by the initial polarization in the x direction. The width is given by the inverse of the time to lose spin coherence, either due to a
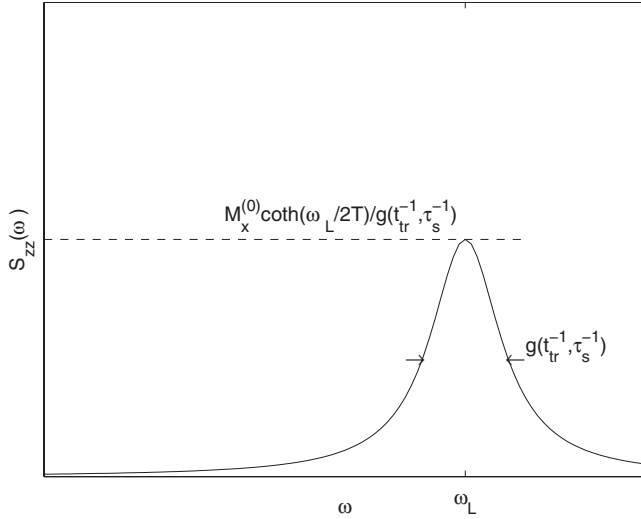
FIG. 2. General qualitative form of the noise-power spectrum. It is peaked at the Larmor frequency ω_L. Its width is approximately equal to the larger of the inverse travel time t_{tr}^{-1} and the inverse spin-decay time τ_s^{-1}. The height is given by the magnetization $M_x^{(0)}$ multiplied by the thermal factor $\coth \omega_L/2T$ and divided by the width.

spin flip or by moving out of the probed region. This inverse time divides the magnetization to give the noise power the dimension of inverse frequency. The peak frequency is determined by the precession in the external magnetic field.

To get a feeling for experimental values of these parameters, we consider their typical values for the spin-noise measurement in lightly n-doped GaAs. The doping level 10^{-16} cm^{-3} gives $E_F = 28$ K. At the helium temperature of 4 K, we are in the degenerate regime with the spin lifetime τ_s about 30 ns. Over the size of the probed region R of 10 μm the electron motion is diffusive with the diffusion constant D of about 5 cm^2/s giving the traveling time t_{tr} of about 200 ns. Thus, a typical spin-noise measurement on n-doped GaAs is done in the degenerate diffusive regime where the spin-flip rate dominates the inverse traveling time out of the probed region. As discussed below, the noise spectrum in this case will have the Lorentzian line shape.

III. IMPLICATIONS

We discuss consequences of Eq. (6). Because $M_x^{(0)}$ grows linearly with the probed volume, and the other quantities in Eq. (6) are independent of L, the height of the power spectrum grows linearly with L while its width is independent of L.

The dependence of the noise-power spectrum on R is different for the ballistic and diffusive motion. In the ballistic case, the height of the noise-power spectrum behaves as

$$S_{zz}(\omega_L) \propto \frac{R^2}{\frac{v}{R} + \tau_s^{-1}} \qquad (10)$$
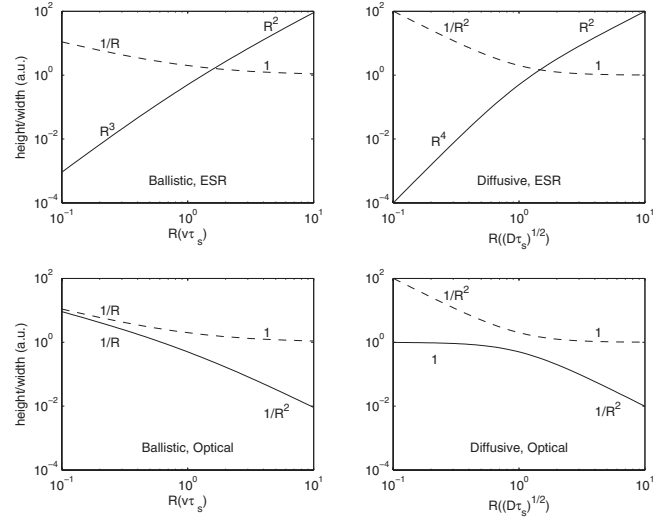
and its width behaves as

FIG. 3. Scaling of the height (solid line) and width (dashed line) of the noise-power spectrum as a function of R in the ESR measurements (first row) and optical measurements (second row). The first row are the log-log plots of formulas (10)–(13); the second row are the log-log plots of the same formulas with the height divided by R^4. The heights and widths are normalized to their value at $R = v\tau_s$ for the ballistic case (the first column) and at $R = \sqrt{D\tau_s}$ for the diffusive case (the second column). The scaling in the different regions is denoted at each curve. The crossover is most pronounced for the optical measurement in the diffusive regime.

$$g(t_{tr}^{-1}, \tau_s^{-1}) \propto \frac{v}{R} + \tau_s^{-1}. \qquad (11)$$

Thus, for $R < v\tau_s$, the height of the noise-power spectrum scales as R^3 and its width as $1/R$, whereas for $R > v\tau_s$, the height of the noise-power spectrum scales as R^2 and its width is independent of R. In the diffusive regime, the height of the noise power spectrum behaves as

$$S_{zz}(\omega_L) \propto \frac{R^2}{\frac{D}{R^2} + \tau_s^{-1}} \qquad (12)$$

and its width behaves as

$$g(t_{tr}^{-1}, \tau_s^{-1}) \propto \frac{D}{R^2} + \tau_s^{-1}. \qquad (13)$$

Thus, for $R < \sqrt{D\tau_s}$, the height of the noise-power spectrum scales as R^4 and its width as $1/R^2$, whereas for $R > \sqrt{D\tau_s}$, the height of the noise power spectrum scales as R^2 and its width is independent of R. For both the ballistic and diffusive transport in the long-R limit, we recover the behavior of static spins flipping on the time scale τ_s. For optical Kerr/Faraday rotation experiments, there is an additional factor $1/A^2$ in the height of the noise-power spectrum for the geometrical factor, Eq. (1). The scaling behavior is summarized in Fig. 3. The scaling crossover is most pronounced in optical measurements of the noise in the diffusive regime.
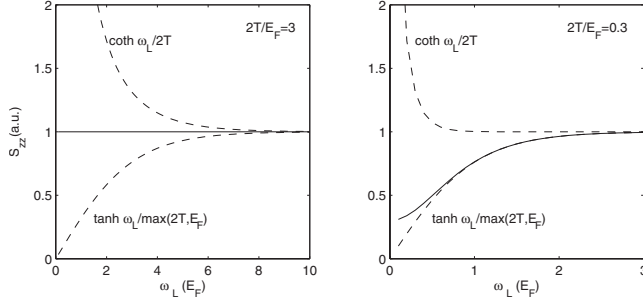
FIG. 4. Solid line: the magnetic-field dependence of the integrated noise-power spectrum S_{zz} in the classical ($2T/E_F = 3$, left panel) and degenerate ($2T/E_F = 0.3$, right panel) regime. Dashed lines: the factors $\coth\frac{\omega_L}{2T}$ (upper dashed lines) and $\tanh\frac{\omega_L}{\max(2T,E_F)}$. The value of S_{zz} is normalized to its value in the high-field limit. In the classical regime, the field dependence of the two factors cancels and S_{zz} is field independent. In the degenerate regime, S_{zz} grows linearly with field in the region $2T < \omega_L < E_F$.

We consider the dependence of the noise-power spectrum on the external magnetic field, that is, on the Larmor frequency ω_L. The width is independent of ω_L. Hence, instead of studying the width and the height of the noise-power spectrum separately, we study the integrated spin-noise-power spectrum

$$S_{zz} \equiv \int_0^\infty d\omega \, S_{zz}(\omega), \tag{14}$$

which scales as the product of the width and the height. From Eq. (6), we see that

$$S_{zz} \propto \coth\frac{\omega_L}{2T} M_x^{(0)}, \tag{15}$$

that is, it is independent of the characteristic rate $g(t_{tr}^{-1}, \tau_s^{-1})$. In the classical regime, the magnetization $M_x^{(0)}$ depends on ω_L as

$$M_x^{(0)} \propto \tanh\frac{\omega_L}{2T}. \tag{16}$$

In the degenerate regime, $M_x^{(0)}$ also has a linear dependence on ω_L for small ω_L cut off at the Fermi energy E_F. We, therefore, approximate the field dependence of $M_x^{(0)}$ by

$$M_x^{(0)} \propto \tanh\frac{\omega_L}{\max(2T,E_F)} \tag{17}$$

giving

$$S_{zz} \propto \coth\frac{\omega_L}{2T}\tanh\frac{\omega_L}{\max(2T,E_F)}. \tag{18}$$

In the classical regime, $2T/E_F > 1$, the ω_L dependence of the two factors in Eq. (18) cancels, and S_{zz} is independent of the magnetic field, in agreement with the measurements of spin noise in Rb vapors.[7] In the degenerate regime, $2T/E_F < 1$, there is an intermediate regime of magnetic fields $2T < \omega_L < E_F$, where S_{zz} grows linearly with field, see Fig. 4.

The spin-noise measurements in GaAs (Refs. 10–12) were done at temperature $T \gg \omega_L$ so S_{zz} is field independent.

IV. CALCULATION

We now turn to a detailed justification of the above results. We calculate the susceptibility χ_{zz} as a linear response of the spin density $\langle s_z(\mathbf{r},t)\rangle$ to an external potential $\phi(\mathbf{r},t)$. The Hamiltonian describing the coupling is

$$H_\phi = \int d^3r \, \phi(\mathbf{r},t) s_z(\mathbf{r},t). \tag{19}$$

In terms of the electron field operator in the Heisenberg representation, $\psi(\mathbf{r},t)$, the spin-density operator $s_z(\mathbf{r},t)$ is given as

$$s_z(\mathbf{r},t) = \psi^\dagger(\mathbf{r},t)\frac{\sigma_z}{2}\psi(\mathbf{r},t), \tag{20}$$

where σ_z is a Pauli matrix. In order to calculate the linear response, we construct and solve the kinetic equation for the density matrix in the Wigner representation

$$\rho_{\alpha\beta}(\mathbf{p},\mathbf{r},t) = \int d^3\tilde{r}\, e^{-i\mathbf{p}\cdot\tilde{\mathbf{r}}}\left\langle \psi_\beta^\dagger\left(\mathbf{r}-\frac{\tilde{\mathbf{r}}}{2},t\right)\psi_\alpha\left(\mathbf{r}+\frac{\tilde{\mathbf{r}}}{2},t\right)\right\rangle. \tag{21}$$

In terms of this density matrix, the spin density is

$$\langle s_z(\mathbf{r},t)\rangle = \int \frac{d^3p}{(2\pi)^3}\text{tr}\left[\rho(\mathbf{p},\mathbf{r},t)\frac{\sigma_z}{2}\right]. \tag{22}$$

The Hamiltonian consists of three terms: a noninteracting term

$$H_0 = \int d^3r\left[\frac{1}{2m}\nabla\psi^\dagger(\mathbf{r},t)\nabla\psi(\mathbf{r},t) - \omega_L\psi^\dagger(\mathbf{r},t)\frac{\sigma_x}{2}\psi(\mathbf{r},t)\right] \tag{23}$$

a coupling term to the external potential in Eq. (19), and a scattering term, which determines whether the particle motion is ballistic or diffusive. The first term on the right-hand side of Eq. (23) is the kinetic energy and the second term describes the interaction with the applied magnetic field. The kinetic equation for the density matrix has the following form:

$$\partial_t \rho_{\alpha\beta}(\mathbf{p},\mathbf{r},t) - i \int d^3\tilde{r} e^{-i\mathbf{p}\cdot\tilde{\mathbf{r}}} \left\langle \left[H_0 + H_\phi, \psi_\beta^\dagger \left(\mathbf{r} - \frac{\tilde{\mathbf{r}}}{2}, t \right) \psi_\alpha \left(\mathbf{r} + \frac{\tilde{\mathbf{r}}}{2}, t \right) \right] \right\rangle = I_s \tag{24}$$

where I_s describes the effect of scattering. Substituting Eqs. (19) and (23) into Eq. (24), we find

$$\left(\partial_t + \frac{\mathbf{p}}{m} \cdot \nabla \right) \rho(\mathbf{p},\mathbf{r},t) - i\omega_L \left[\frac{\sigma_x}{2}, \rho(\mathbf{p},\mathbf{r},t) \right] - i \left[\phi\left(\mathbf{r} - \frac{i}{2}\partial_{\mathbf{p}}, t \right) \rho(\mathbf{p},\mathbf{r},t) \frac{\sigma_z}{2} - \phi\left(\mathbf{r} + \frac{i}{2}\partial_{\mathbf{p}}, t \right) \frac{\sigma_z}{2} \rho(\mathbf{p},\mathbf{r},t) \right] = I_s. \tag{25}$$

To obtain linear response, we write

$$\rho(\mathbf{p},\mathbf{r},t) = \rho^{(0)}(p) + \delta\rho(\mathbf{p},\mathbf{r},t). \tag{26}$$

Here, $\rho^{(0)}(p)$ is the equilibrium density matrix corresponding to the Hamiltonian H_0, that is,

$$\rho^{(0)}(p) = \frac{1}{2} \left[n\left(\xi(p) - \frac{\omega_L}{2} \right) + n\left(\xi(p) + \frac{\omega_L}{2} \right) \right] \sigma_0$$
$$+ \frac{1}{2} \left[n\left(\xi(p) - \frac{\omega_L}{2} \right) - n\left(\xi(p) + \frac{\omega_L}{2} \right) \right] \sigma_x$$
$$\equiv \rho_0^{(0)}(p)\sigma_0 + \rho_x^{(0)}(p)\sigma_x. \tag{27}$$

Here

$$n(\xi) = \frac{1}{e^{(\xi-\mu)/T} + 1} \tag{28}$$

is the Fermi-Dirac distribution function and

$$\xi(p) = \frac{p^2}{2m} \tag{29}$$

is the band dispersion. The particular deviations from equilibrium we consider have the form

$$\delta\rho(\mathbf{p},\mathbf{r},t) = \delta\rho_y(\mathbf{p},\mathbf{r},t)\sigma_y + \delta\rho_z(\mathbf{p},\mathbf{r},t)\sigma_z \equiv \delta\boldsymbol{\rho}(\mathbf{p},\mathbf{r},t) \cdot \boldsymbol{\sigma}. \tag{30}$$

The scattering contribution to the kinetic equation is different for the ballistic and diffusive motion. We first consider the case of the ballistic motion, in which

$$I_s = -\frac{1}{\tau_s} \delta\rho(\mathbf{p},\mathbf{r},t). \tag{31}$$

It describes spin relaxation with relaxation time τ_s.

To obtain the susceptibility at positive frequencies, we write the kinetic equation for the circular component of the density matrix

$$\delta\rho_+(\mathbf{p},\mathbf{q},\omega) = \int d^3r\, dt\, e^{-i\mathbf{q}\cdot\mathbf{r}+i\omega t}(\delta\rho_z - i\delta\rho_y)(\mathbf{p},\mathbf{r},t). \tag{32}$$

The equation for the opposite circular component $\delta\rho_-$ gives the susceptibility at negative frequencies, which gives an equivalent result. The kinetic equation becomes

$$-i\left(\omega - \omega_L - \frac{\mathbf{p}}{m}\cdot\mathbf{q} + \frac{i}{\tau_s} \right) \delta\rho_+^B(\mathbf{p},\mathbf{q},\omega) = i\phi(\mathbf{q},\omega) \frac{\rho_0^{(0)}\left(\mathbf{p}+\frac{\mathbf{q}}{2}\right) - \rho_0^{(0)}\left(\mathbf{p}-\frac{\mathbf{q}}{2}\right) - \rho_x^{(0)}\left(\mathbf{p}+\frac{\mathbf{q}}{2}\right) - \rho_x^{(0)}\left(\mathbf{p}-\frac{\mathbf{q}}{2}\right)}{2}. \tag{33}$$

The superscript B denotes the case of ballistic motion. To obtain the susceptibility, we solve for

$$\delta\rho_+^B(\mathbf{q},\omega) = \int \frac{d^3p}{(2\pi)^3} \delta\rho_+^B(\mathbf{p},\mathbf{q},\omega), \tag{34}$$

which gives, using Eq. (22)

$$\chi_{zz}^B(q,\omega > 0) = \frac{1}{4} \int \frac{d^3p}{(2\pi)^3} \frac{n\left(\xi\left(\mathbf{p} - \frac{\mathbf{q}}{2} \right) - \frac{\omega_L}{2} \right) - n\left(\xi\left(\mathbf{p} + \frac{\mathbf{q}}{2} \right) + \frac{\omega_L}{2} \right)}{\omega - \omega_L - \frac{\mathbf{p}}{m}\cdot\mathbf{q} + \frac{i}{\tau_s}}. \tag{35}$$

For diffusive motion, the fermion momentum relaxes on a rapid time scale $\tau \ll \tau_s$. In this case, the scattering contribution to the kinetic equation is

$$I_s = -\frac{1}{\tau_s}\delta\rho(\mathbf{p},\mathbf{r},t) - \frac{1}{\tau}[\rho(\mathbf{p},\mathbf{r},t) - \rho_{eq}(p;\rho(\mathbf{r},t))], \quad (36)$$

where $\rho_{eq}(p;\rho(\mathbf{r},t))$ is the momentum equilibrium distribution consistent with the local number-spin density $\rho(\mathbf{r},t)$

$$\int \frac{d^3p}{(2\pi)^3}\rho_{eq}(p;\rho(\mathbf{r},t)) = \rho(\mathbf{r},t). \quad (37)$$

For $\delta\rho(\mathbf{p},\mathbf{r},t)$ given by Eq. (30)

$$I_s = -\frac{1}{\tau_s}\delta\rho(\mathbf{p},\mathbf{r},t) - \frac{1}{\tau}\delta\rho(\mathbf{p},\mathbf{r},t)$$

$$+ \frac{1}{\tau}\frac{n\left(\xi(p) - \frac{\omega_L}{2}\right) - n\left(\xi(p) + \frac{\omega_L}{2}\right)}{\int \frac{d^3p}{(2\pi)^3}\left[n\left(\xi(p) - \frac{\omega_L}{2}\right) - n\left(\xi(p) + \frac{\omega_L}{2}\right)\right]}\delta\rho(\mathbf{r},t). \quad (38)$$

To obtain the susceptibility at positive frequencies, we write the kinetic equation for the circular component of the density matrix

$$-i\left(\omega - \omega_L - \frac{\mathbf{p}}{m}\cdot\mathbf{q} + \frac{i}{\tau_s} + \frac{i}{\tau}\right)\delta\rho_+^D(\mathbf{p},\mathbf{q},\omega) = i\phi(\mathbf{q},\omega)\frac{\rho_0^{(0)}\left(\mathbf{p}+\frac{\mathbf{q}}{2}\right) - \rho_0^{(0)}\left(\mathbf{p}-\frac{\mathbf{q}}{2}\right) - \rho_x^{(0)}\left(\mathbf{p}+\frac{\mathbf{q}}{2}\right) - \rho_x^{(0)}\left(\mathbf{p}-\frac{\mathbf{q}}{2}\right)}{2}$$

$$+ \frac{1}{\tau}\frac{n\left(\xi(p) - \frac{\omega_L}{2}\right) - n\left(\xi(p) + \frac{\omega_L}{2}\right)}{\int \frac{d^3p}{(2\pi)^3}\left[n\left(\xi(p) - \frac{\omega_L}{2}\right) - n\left(\xi(p) + \frac{\omega_L}{2}\right)\right]}\delta\rho_+^D(\mathbf{q},\omega). \quad (39)$$

The superscript D denotes the case of diffusive motion. To obtain the susceptibility, we solve for

$$\delta\rho_+^D(\mathbf{q},\omega) = \int \frac{d^3p}{(2\pi)^3}\delta\rho_+^D(\mathbf{p},\mathbf{q},\omega), \quad (40)$$

which to lowest order in τ gives, using Eq. (22)

$$\chi_{zz}^D(q,\omega > 0) = \frac{1}{4}\frac{\int \frac{d^3p}{(2\pi)^3}\left[n\left(\xi(\mathbf{p}) - \frac{\omega_L}{2}\right) - n\left(\xi(\mathbf{p}) + \frac{\omega_L}{2}\right)\right]}{\omega - \omega_L + i[\tau_s^{-1} + D(\omega_L)q^2]}. \quad (41)$$

Here

$$D(\omega_L) = \tau\frac{\int \frac{d^3p}{(2\pi)^3}\frac{p^2}{3m^2}\left[n\left(\xi(\mathbf{p}) - \frac{\omega_L}{2}\right) - n\left(\xi(\mathbf{p}) + \frac{\omega_L}{2}\right)\right]}{\int \frac{d^3p}{(2\pi)^3}\left[n\left(\xi(\mathbf{p}) - \frac{\omega_L}{2}\right) - n\left(\xi(\mathbf{p}) + \frac{\omega_L}{2}\right)\right]}. \quad (42)$$

In the limit $\omega_L \to 0$, $D(\omega_L)$ is equal to the usual diffusion constant. For the classical distribution $n(\xi)$ in the high-temperature limit, $D(\omega_L)$ is independent of ω_L for any value of ω_L. At $T=0$, the high-field limit $D(\omega_L/2 > E_F)$ is reduced compared to the low-field limit $D(\omega_L \to 0)$ by a factor of $2^{2/3} \times 3/5 = 0.95$. Thus we consider D independent of the magnetic field and drop the ω_L dependence in the following.

Substituting Eq. (35) into Eq. (4) gives

$$S_{zz}^B(\omega) \simeq \frac{\pi}{2}\coth\frac{\omega}{2T}A \times L\int \frac{d^3p}{(2\pi)^3}\left[\frac{n\left(\xi\left(\mathbf{p}-\frac{\mathbf{e}}{2R}\right) - \frac{\omega_L}{2}\right) - n\left(\xi\left(\mathbf{p}+\frac{\mathbf{e}}{2R}\right) + \frac{\omega_L}{2}\right)}{2}\right]\frac{\frac{1}{\pi\tau_s}}{\left(\omega - \omega_L - \frac{\mathbf{p}}{m}\cdot\frac{\mathbf{e}}{R}\right)^2 + \frac{1}{\tau_s^2}} \quad (43)$$

for the case of the ballistic motion. Here $\mathbf{e}$ is the unit vector in an arbitrary direction. Substituting Eq. (41) into Eq. (4) gives

$$S_{zz}^D(\omega) \simeq \frac{\pi}{2}\coth\frac{\omega}{2T}A \times L \int \frac{d^3p}{(2\pi)^3}\left[\frac{n\left(\xi(\mathbf{p}) - \frac{\omega_L}{2}\right) - n\left(\xi(\mathbf{p}) + \frac{\omega_L}{2}\right)}{2}\right]\frac{\frac{1}{\pi}(\tau_s^{-1} + D/R^2)}{(\omega - \omega_L)^2 + (\tau_s^{-1} + D/R^2)^2} \tag{44}$$

for the case of the diffusive motion. Evaluating the integrals in Eqs. (43) and (44), see Appendix B, gives results of the form of Eq. (6), with specific forms for function $f((\omega - \omega_L)/g(t_{tr}^{-1}, \tau_s^{-1}))$. The forms of the function f in the various cases are summarized in Table I.

In the diffusive case, the function f is a Lorentzian for all temperatures and

$$g(t_{tr}^{-1}, \tau_s^{-1}) = t_{tr}^{-1} + \tau_s^{-1}. \tag{45}$$

The function f in the ballistic case in Eq. (35) is more complicated so we consider various limiting cases. In the limit $\tau_s^{-1} \gg v/R$, where v is the Fermi velocity at $T=0$ and the thermal velocity $\sqrt{2T/m}$ at $T > E_F$, we can drop $\mathbf{p}/m \cdot \mathbf{q}$ from the denominator of Eq. (35), so the numerator becomes q independent, and we obtain a Lorentzian with the width τ_s^{-1}, like in the diffusive regime for $\tau_s^{-1} \gg D/R^2$. In the limit of τ_s^{-1} dominating the inverse travel time through the probed region, the spin noise can not distinguish between the ballistic motion and diffusive motion. We can distinguish between these cases in the opposite limit $\tau_s^{-1} \to 0$. Then the line in the diffusive regime is still a Lorentzian but now with the width D/R^2. In the ballistic case, at $T=0$, the line has a trapezoidal shape for $\omega_L \ll E_F$ and a parabolic shape for $\omega_L \gg E_F$. In the classical limit $T \gg E_F$, the line has a Gaussian shape.

V. CONCLUSIONS

Motivated by spin-noise spectroscopy measurements, we developed a theory of spin noise of itinerant fermions in different regimes of temperature and disorder. We found a general result with a clear physical interpretation and showed how it follows from spin kinetic equations. Our theory provides a framework for interpreting recent experiments on atomic gases and conduction electrons in semiconductors and provides a baseline for identifying the effects of interactions on spin-noise spectroscopy.

TABLE I. Summary of the shapes of the noise spectral lines in the four regimes in the limit $\tau_s^{-1} \to 0$.

	$R < v\tau$ (ballistic)	$R > v\tau$ (diffusive)
$T < E_F$ (degenerate)	Trapezoidal (for $\omega_L/2 < E_F$) Parabolic (for $\omega_L/2 > E_F$)	Lorentzian
$T > E_F$ (classical)	Gaussian	Lorentzian

APPENDIX A

In this appendix, we derive the spin-noise-power spectrum $S_{zz}(\omega)$ for a single spin J in the magnetic field applied in the x direction

$$S_{zz}(t_2 - t_1) \equiv \frac{1}{2}\langle\{J_z(t_2), J_z(t_1)\}\rangle$$

$$= \frac{1}{8}(e^{-i\omega_L(t_2-t_1)} + e^{i\omega_L(t_2-t_1)})\langle\{J_+, J_-\}\rangle, \tag{A1}$$

where

$$J_\pm = J_z \mp iJ_y. \tag{A2}$$

The thermal expectation value of the anticommutator is related to the thermal expectation value of the commutator

$$\langle\{J_+, J_-\}\rangle = \coth\frac{\omega_L}{2T}\langle[J_+, J_-]\rangle. \tag{A3}$$

Using the commutation relation

$$[J_+, J_-] = 2J_x \tag{A4}$$

we arrive at the result

$$S_{zz}(\omega > 0) = \frac{\pi}{2}\coth\frac{\omega_L}{2T}\langle J_x\rangle\delta(\omega - \omega_L). \tag{A5}$$

We see that Eq. (A5) has the form of Eq. (6) with

$$\frac{1}{g(t_{tr}^{-1}, \tau_s^{-1})}f\left(\frac{\omega - \omega_L}{g(t_{tr}^{-1}, \tau_s^{-1})}\right) = \delta(\omega - \omega_L). \tag{A6}$$

The formula for magnetization

$$\langle J_x\rangle = \frac{2J+1}{2}\coth\frac{(2J+1)\omega_L}{2T} - \frac{1}{2}\coth\frac{\omega_L}{2T} \tag{A7}$$

implies that in the special case of $J=1/2$, the temperature and field dependence cancels between $\coth\omega_L/2T$ and $\langle J_x\rangle$ giving

$$S_{zz}(\omega > 0) = \frac{\pi}{4}\delta(\omega - \omega_L). \tag{A8}$$

APPENDIX B

We present the details of calculations for the ballistic case with $\tau_s^{-1} \to 0$ in three different limiting cases.

1. $T=0$, $\omega_L \ll E_F$

In this case, we can linearize around the Fermi surface. From Eq. (35), we now get

$$
\chi_B''(q, \omega > 0) = -\frac{\pi}{4} N_0 \int d\xi \int_{-1}^{1} \frac{dc}{2} \left[\theta\left(-\xi + \frac{v_F qc + \omega_L}{2}\right) \right.
$$
$$
\left. - \theta\left(-\xi - \frac{v_F qc + \omega_L}{2}\right) \right] \delta[\omega - (v_F qc + \omega_L)]
$$
$$
\simeq -\frac{\pi}{2} \times \frac{N_0 \omega_L}{2} \times \frac{\omega}{\omega_L} \frac{\theta(v_F q - |\omega - \omega_L|)}{2 v_F q}. \quad \text{(B1)}
$$

We thus obtain Eq. (6) with the magnetization proportional to the magnetic field via the Pauli susceptibility, $M_x^{(0)} = N_0 \omega_L / 2$, ballistic transport time $t_{tr} = R/v_F$, and f with a trapezoidal shape.

2. $T=0$, $\omega_L/2 > E_F$

In this case, the fermions are fully polarized so

$$
\chi_B''(q, \omega > 0) = -\frac{\pi}{4} \int_0^{\infty} \frac{p^2 dp}{(2\pi)^2} \int_{-1}^{1} dc\, \delta\left(\omega - \omega_L - \frac{p}{m} qc\right)
$$
$$
\times \theta\left[\mu + \frac{1}{2}\left(\omega_L - \frac{p}{m} qc\right) - \frac{p^2 + (q/2)^2}{2m}\right]
$$
$$
\simeq -\frac{1}{16\pi} \frac{m^2}{q} \int_{(\omega - \omega_L)^2 m/2q^2}^{\infty} d\epsilon\, \theta\left(\mu + \frac{\omega}{2} - \epsilon\right),
$$
$$
\quad \text{(B2)}
$$

where we neglected $q^2/2m$ compared to the Fermi energy $\mu + \omega_L/2$ because the size of the probed region is much larger than the Fermi wavelength. Using the formula for particle density

$$
n = \frac{1}{6\pi^2} p_F^3 \quad \text{(B3)}
$$

with

$$
p_F = \sqrt{2m\left(\mu + \frac{\omega_L}{2}\right)}, \quad \text{(B4)}
$$

we find

$$
\chi_B''(q, \omega > 0) = -\frac{\pi}{2} \times \frac{n}{2} \times \frac{3}{4} \frac{1}{q p_F/m} \left[1 - \left(\frac{\omega - \omega_L}{q p_F/m}\right)^2\right]. \quad \text{(B5)}
$$

The magnetization is now saturated at one-half times the number of the fermions in the probed region. The susceptibility is nonzero because it is transverse to the external magnetic field (zz response function with the external magnetic field applied in the x direction). The transport time is still equal to R/v_F. The line shape f is now parabolic.

3. $T > E_F$

In this case, we approximate

$$
n(\xi) = e^{-(\xi - \mu)/T} \quad \text{(B6)}
$$

with $\mu < 0$ so Eq. (6) gives

$$
\chi_B''(q, \omega > 0) = -\frac{\pi}{8} n \frac{\displaystyle\int_0^{\infty} p^2 dp \int_{-1}^{1} dc\, e^{-[p^2 + (q/2)^2]/2mT} \sinh\left(\frac{pqc/m - \omega_L}{2T}\right) \delta(\omega - (pqc/m - \omega_L))}{\displaystyle\int_0^{\infty} p^2 dp\, e^{-p^2/2mT} \cosh\frac{\omega_L}{2T}}
$$
$$
\simeq -\frac{\pi}{2} \times \frac{n}{2} \tanh\frac{\omega_L}{2T} \times \frac{e^{-(\omega - \omega_L)^2/2Tq^2/m}}{\sqrt{2\pi Tq^2/m}}. \quad \text{(B7)}
$$

Thus, the equilibrium magnetization is $n/2 \tanh \omega_L/2T$, the transport time is R/v, where v is the thermal velocity $\sqrt{2T/m}$ and the line shape f is Gaussian.

*simonkos@kfy.zcu.cz

[1] T. Sleator, E. L. Hahn, C. Hilbert, and J. Clarke, Phys. Rev. Lett. **55**, 1742 (1985).

[2] M. B. Weissman, Rev. Mod. Phys. **65**, 829 (1993).

[3] N. Smith and P. Arnett, Appl. Phys. Lett. **78**, 1448 (2001).

[4] S. Crooker, J. Brandt, C. Sanfort, A. Greilich, D. Yakovlev, D.

Reuter, A. Wieck, and M. Bayer, Phys. Rev. Lett. **104**, 036601 (2010).

[5] E. B. Aleksandrov and V. S. Zapassky, Zh. Eksp. Teor. Fiz. **81**, 132 (1981) [Sov. Phys. JETP **54**, 64 (1981)].

[6] T. Mitsui, Phys. Rev. Lett. **84**, 5292 (2000).

[7] S. A. Crooker, D. G. Rickel, A. V. Balatsky, and D. L. Smith,

Nature (London) **431**, 49 (2004).

[8] J. L. Sorensen, J. Hald, and E. S. Polzik, Phys. Rev. Lett. **80**, 3487 (1998).

[9] A. Kuzmich, L. Mandel, J. Janis, Y. E. Young, R. Ejnisman, and N. P. Bigelow, Phys. Rev. A **60**, 2346 (1999).

[10] M. Oestreich, M. Römer, R. J. Haug, and D. Hägele, Phys. Rev. Lett. **95**, 216603 (2005).

[11] S. A. Crooker, L. Cheng, and D. L. Smith, Phys. Rev. B **79**, 035208 (2009).

[12] G. M. Müller, M. Römer, D. Schuh, W. Wegscheider, J. Hübner, and M. Oestreich, Phys. Rev. Lett. **101**, 206601 (2008).

[13] Y. Manassen, R. J. Hamers, J. E. Demuth, and A. J. Castellano, Jr., Phys. Rev. Lett. **62**, 2531 (1989).

[14] A. V. Balatsky, Y. Manassen, and R. Salem, Phys. Rev. B **66**, 195416 (2002).

[15] M. Römer, J. Hübner, and M. Oestreich, Rev. Sci. Instrum. **78**, 103903 (2007).

[16] M. Römer, J. Hübner, and M. Oestreich, Appl. Phys. Lett. **94**, 112105 (2009).